Biochimica et Biophysica Acta 1828 (2013) 2720–2728

Contents lists available at ScienceDirect

Biochimica et Biophysica Acta

journal homepage: www.elsevier.com/locate/bbamem

Correlations between membrane immersion depth, orientation, and salt-resistance of tryptophan-rich antimicrobial peptides

Hui-Yuan Yu [a,1], Bak-Sau Yip [a,b,1], Chih-Hsiang Tu [a], Heng-Li Chen [a], Hung-Lun Chu [a], Ya-Han Chih [a], Hsi-Tsung Cheng [a], Shih-Che Sue [c,*], Jya-Wei Cheng [a,*]

[a] Institute of Biotechnology and Department of Medical Science, National Tsing Hua University, Hsinchu 300, Taiwan
[b] Department of Neurology, National Taiwan University Hospital Hsinchu Branch, Hsinchu 300, Taiwan
[c] Institute of Bioinformatics and Structural Biology and Department of Life Science, National Tsing Hua University, Hsinchu 300, Taiwan

ARTICLE INFO

Article history:
Received 22 March 2013
Received in revised form 1 July 2013
Accepted 15 July 2013
Available online 27 July 2013

Keywords:
Antimicrobial peptide
Tryptophan-rich
Salt-resistance
NMR
PRE

ABSTRACT

The efficacies of many antimicrobial peptides are greatly reduced in the presence of high salt concentrations therefore limiting their development as pharmaceutical compounds. PEM-2-W5K/A9W, a short Trp-rich antimicrobial peptide developed based on the structural studies of PEM-2, has been shown to be highly active against various bacterial strains with less hemolytic activity. Here, correlations between membrane immersion depth, orientation, and salt-resistance of PEM-2 and PEM-2-W5K/A9W have been investigated via solution structure and paramagnetic resonance enhancement studies. The antimicrobial activities of PEM-2-W5K/A9W and PEM-2 against various bacterial and fungal strains including multidrug-resistant and clinical isolates under high salt conditions were tested. The activities of the salt-sensitive peptide PEM-2 were reduced and diminished at high salt concentrations, whereas the activities of PEM-2-W5K/A9W were less affected. The results indicated that the strong salt-resistance of PEM-2-W5K/A9W may arise from the peptide positioning itself deeply into microbial cell membranes and thus able to disrupt the membranes more efficiently.

1. Introduction

Current treatments for bacterial and fungal infections are hindered by issues such as ineffective elimination of infections, serious side effects, and emerging drug resistant microbes. As the prevalence of bacterial and fungal resistant strains increases significantly, it is urgent to have new alternatives at hands [1]. Antimicrobial peptides are found to be important in the host innate defense mechanism. Most of the antimicrobial peptides do not target specific molecular receptors, but rather interact and permeabilize microbial membranes [1]. To date, there are thousands of antimicrobial peptides that have been discovered, characterized, and designed. In vitro and in vivo studies have shown that these antimicrobial peptides exhibit a wide range of activity against many disease related microbial organisms [1].

The development of antimicrobial peptides has been hindered by several problems. One of these major problems is salt sensitivity [2]. It was found that the efficacy of the antimicrobial peptide human β-defensin-1 is greatly reduced in the presence of high salt concentrations in bronchopulmonary fluids in cystic fibrosis patients [3]. Similar problems were observed in the clinically active histidine-rich peptide P-113, the Trp-rich peptide indolicidins, gramicidins, bactenecins, and magainins [4–7]. Studies have been reported on the design of salt-resistant antimicrobial peptides. However, most of them were focused on overall structure modifications [2,4,8–12].

Previously, a series of short peptides with improved antimicrobial activities were designed based on the Trp-rich antimicrobial peptide PEM-2 (KKWRWWLKALAKK) [13]. Of these newly designed peptides, PEM-2-W5K, with Trp5 of PEM-2 replaced by Lys, was found to have similar MIC values compared with those of PEM-2 but possesses a lower human red blood cell hemolytic activity [14]. PEM-2-W5A/A9W, with residues Trp5 and Ala9 of PEM-2 swapping positions, has 2–8 times more potent antimicrobial activities than PEM-2. However, an increase of hemolysis of human red blood cells was also found. PEM-2-W5K/A9W, with Trp5 and Ala9 replaced by Lys and Trp, was then designed based on the studies of PEM-2, PEM-2-W5K, and PEM-2-W5A/A9W [14].

Although PEM-2-W5K/A9W is highly active against various bacterial strains and possesses less hemolytic activity, many questions still remain to be elucidated. For example, what are the changes of the structural features between PEM-2-W5K/A9W and PEM-2? Are these structural changes affecting the peptide-membrane interaction hence affecting its antimicrobial activities under high salt conditions? Can we design new types of Trp-rich antimicrobial peptides based on the structural and peptide-membrane interaction studies of PEM-2 and PEM-2-W5K/A9W? Information about

* Corresponding authors. Tel.: +886 3 5742763, +886 3 5742025; fax: +886 3 5715934.
E-mail addresses: scsue@life.nthu.edu.tw (S.-C. Sue), jwcheng@life.nthu.edu.tw (J.-W. Cheng).
[1] Contributed equally to this paper.

0005-2736/$ – see front matter © 2013 Elsevier B.V. All rights reserved.
http://dx.doi.org/10.1016/j.bbamem.2013.07.020

the peptide–membrane interaction such as membrane immersion depth and orientation of antimicrobial peptides can be obtained by measuring paramagnetic relaxation enhancement (PRE) using various paramagnetic compounds. For example, the orientation of the α-helical peptide CM-15 in DPC micelles was accurately measured via experimental PREs using the water-soluble paramagnetic relaxation agent gadolinium-diethylenetriamine pentaacetic acid-bismethylamide Gd(DTPA-BMA) [15]. On the other hand, the positioning of the peptides in the interior of the DPC micelle can be measured using the paramagnetic probe 16-doxylstearic acid [16,17]. Broadening and decreasing of NMR signals can be observed from residues outside the micelle in the presence of Gd(DTPA-BMA), or deeply buried in the micelle in the presence of 16-doxylstearic acid. In here, we have used solution NMR and paramagnetic relaxation enhancement techniques to study the structural features of PEM-2-W5K/A9W and DPC micelle interactions. The results are compared with the peptide–micelle interactions of the parent peptide PEM-2. Moreover, the antimicrobial activities of PEM-2-W5K/A9W against various bacterial and fungal strains including multidrug-resistant and clinical isolates under high salt conditions are tested. Correlations between membrane immersion depth, orientation, and salt resistance of these peptides are discussed.

2. Materials and methods

2.1. Sample preparation

All of the peptide samples were purchased from SynBioSci (Livermore, CA). The identity of the peptides was checked by electrospray mass spectroscopy and the purity (>95%) was assessed by HPLC. Peptide concentration was determined by using the UV spectrophotometer at 280 nm. All of the samples were prepared from a stock solution containing PEM-2 or PEM-2-W5K/A9W. In addition, d_{38}-DPC and paramagnetic agents were prepared from stock solutions. The peptides, micelles, and paramagnetic agents were divided into equal amounts in NMR tubes for experiments so that no errors in attenuation factors due to concentration effects occurred.

2.2. NMR Spectroscopy and Structural Calculations

All NMR experiments were performed on a Bruker Avance 600 MHz spectrometer at 37 °C using a 2 mM sample. NOESY spectra were acquired at four different mixing times of 60, 90, 120, and 250 ms. TOCSY spectra were recorded using the MLEV17 pulse sequence with mixing times of 35 and 70 ms at 2048 points in t2 and 512 points in t1. All chemical shifts were referenced to internal 2,2-dimethyl-2-silapentane-5-sulfonate (DSS).

To avoid spin diffusion problems, distance restraints were acquired from NOEs assigned in a 2D NOESY spectrum with 60 ms mixing time. The NOE cross-peak intensities were classified as strong, medium, and weak, corresponding to distance limits of 1.8–2.8 Å, 2.8–3.6 Å, and 3.6–5.0 Å, respectively. Structural calculations were carried out with the programs CNS 1.2 (A. T. Brünger, Yale University) on a workstation. The final 20 structures contained no distance constraint violations greater than 0.2 Å. An average structure was calculated by averaging the 20 structures, which was refined using the refine.inp protocol as mentioned above. The structures were analyzed with MOLMOL and PROCHECK-NMR [18].

2.3. Paramagnetic relaxation enhancements

The localizations of peptides in DPC micelles were studied by two spin labeled paramagnetic compounds 16-doxyl-stearic acid (16-DSA), and gadolinium-diethylenetriamine pentaacetic acid-bismethylamide, Gd(DTPA-BMA). Paramagnetic probes induced resonance perturbation experiments were performed by acquiring 2-D ^1H–^1H TOCSY spectra (mixing time = 70 ms) in the absence and presence of 2 mM paramagnetic agents. Cross-peak intensities in the fingerprint region were compared. The results are reported in terms of the remaining amplitudes (RA) of the cross-peaks, defined as RA = A(probe)/A(0), where A(probe) is the amplitude of the cross-peak measured when the paramagnetic agent is added and A(0) is the amplitude in the absence of the paramagnetic agent. TOCSY spectra and Gd(DTPA-BMA) attenuated TOCSY spectra of PEM-2 and PEM-2-W5K/A9W are provided in supplementary materials to illustrate the attenuation of the paramagnetic agents.

2.4. Saturation transfer difference studies

For STD-NMR studies, 2 mM peptides were added in 20 mM sodium phosphate buffer in D_2O. DPC was saturated at 1.325 ppm (40.0 ppm for reference) with a cascade of 40 selective Gaussian-shaped pulses (49 ms each) in an interval of 1 ms resulting in total saturation time of 0.5 s in one- and two-dimensional STD experiments. 2D Saturation transfer difference TOCSY spectra were used to detect cross-peaks between the fatty acyl chains of DPC micelles and the aromatic protons of peptides. As a control, 1D and 2D STD experiments were performed by using an identical experimental setup with the same peptide concentration but in perdeuterated dodecylphosphocholine (d_{38}-DPC).

2.5. Bacterial and fungal strains

Escherichia coli strain (ATCC 25922), *Staphylococcus aureus* subsp strain (ATCC 25923, methicillin-resistant), *Staphylococcus aureus* subsp strain (ATCC 29213, methicillin-resistant), *Staphylococcus aureus* subsp strain (ATCC 19636, methicillin-resistant), *Pseudomonas aeruginosa* Migula strain (ATCC 27853, ampicillin-resistant) and *Pseudomonas aeruginosa* Migula strain (ATCC 9027, ampicillin-resistant) were used to test the antibacterial activity of the peptides. Fungal strains from American Type Culture Collection and clinical isolates were used in the anti-Candida experiments. Species identification of the clinical yeast strains has previously been described [6].

2.6. Antimicrobial assays

The antibacterial activities of P-113, PEM-2, and PEM-2-W5K/A9W were determined by the standard broth microdilution method of National Committee for Clinical Laboratory Standards with Mueller–Hinton broth and LYM broth. The anti-Candida activities of fluconazole, P-113, PEM-2, and PEM-2-W5K/A9W were determined in LYM broth media with different salt concentrations. The LYM broth contains 5.4 mM KCl, 5.6 mM Na_2HPO_4, 0.5 mM $MgSO_4$, and 1.0 mM sodium citrate [5]. In addition, 0.4 mg of $ZnCl_2$, 2.0 mg of $FeCl_3 \cdot 6H_2O$, 0.1 mg of $CuSO_4 \cdot 5H_2O$, 0.1 mg of $MnSO_4 \cdot H_2O$, 0.1 mg of $Na_2B_4O_7 \cdot 10H_2O$, 700 mg of amino acid mixtures without tryptophan (Clontech), and 20 mg of L-Tryptophan were added per liter of medium. A vitamin mixture (100×, Sigma) and glucose at final concentration of 2% were also added. The MIC value is the lowest concentration of peptide at which there was no change in optical density. All tests were measured in triplicate. The MIC values were converted to a color scale and displayed using the TreeView Program [19,20]. The hemolytic activities of the peptides were determined from hemolysis against human red blood cells (hRBC) as described previously [21].

3. Results

3.1. Structure calculation and description

Two-dimensional ^1H NMR was used to study the structure PEM-2-W5K/A9W in d_{38}-DPC micelles. The chemical shift assignments of PEM-2-W5K/A9W (2 mM) in 20 mM sodium phosphate buffer (pH 4.5) and in d_{38}-DPC (120 mM) at 37 °C were performed by the standard sequential assignment procedures [22]. Assignments of all

the proton chemical shifts were accomplished by using the TOCSY and NOESY spectra. DQF-COSY was used to assign the Hδ and Hγ in residues. Many of the chemical shifts observed deviated significantly from the random coil values. A total of 385 NOE-derived distance constraints, including 216 intraresidue, 97 sequential, and 72 medium range distance restraints were used in the structure calculations. Among these 385 NOEs, there are 28 redundant NOEs. The overlay of the backbone atoms for the 20 lowest energy structures of PEM-2-W5K/A9W in d_{38}-DPC is shown in Fig. 1A. Fig. 1B shows the final refined averaged structure of PEM-2-W5K/A9W. The electrostatic surface plots of PEM-2-W5K/A9W computed using MOLMOL is shown in Fig. 1C to illustrate the charge distribution of PEM-2-W5K/A9W. The energetic and structural statistics are listed in Table 1. The RMSD calculated from the averaged coordinates for PEM-2-W5K/A9W is 0.26 Å for the backbone heavy atoms (N, C, and Cα) and 1.32 Å for all heavy atoms. Analysis of ϕ and ψ backbone angles is facilitated by using the program Procheck NMR [18]. 91.4% of the residues are within most favored regions and 8.6% of the residues are in additional allowed regions of the Ramachandran plot indicating the correctness of the structure.

The d_{38}-DPC micelle-bound structure of PEM-2-W5K/A9W is similar to the structure of PEM-2 [14] and displays a helical structure with an apparent amphipathic conformation. A cationic amphipathic structure would be best suited for maximizing both electrostatic and hydrophobic interactions with a membrane. The positively charged residues (Lys1, Lys2, Arg4, Lys5, Lys8, Lys12, and Lys13) form a hydrophilic patch. Hydrophobic residues including Trp3, Trp6, Leu7, Trp9, Leu10, and Ala11 form a hydrophobic face.

In addition to the NMR studies, we have conducted circular dichroism (CD) studies of PEM-2 and PEM-2-W5K/A9W under low and high salt conditions in solution (Supplementary materials). The peptide–micelle interactions of PEM-2 and PEM-2-W5K/A9W under low and high salt conditions were also studied by CD. The CD results indicated that there were no apparent structural changes for both PEM-2 and PEM-2-W5K/A9W in solution or in the peptide–micelle interactions under low and high salt conditions. Hence, the membrane insertion depth of PEM-2 and PEM-2-W5K/A9W may not change under various salt concentrations. The salt dependence of peptide self-association in solution and in peptide–micelle interactions for both PEM-2 and PEM-2-W5K/A9W was further studied by 1D NMR linewidth analysis with peptide concentrations ranging from 0.2 mM to 2 mM. There were no noticeable linewidth changes for both peptides under low and high salt conditions in solution. Similarly, no apparent line width changes were found for both peptides in peptide–micelle interactions under low and high salt conditions.

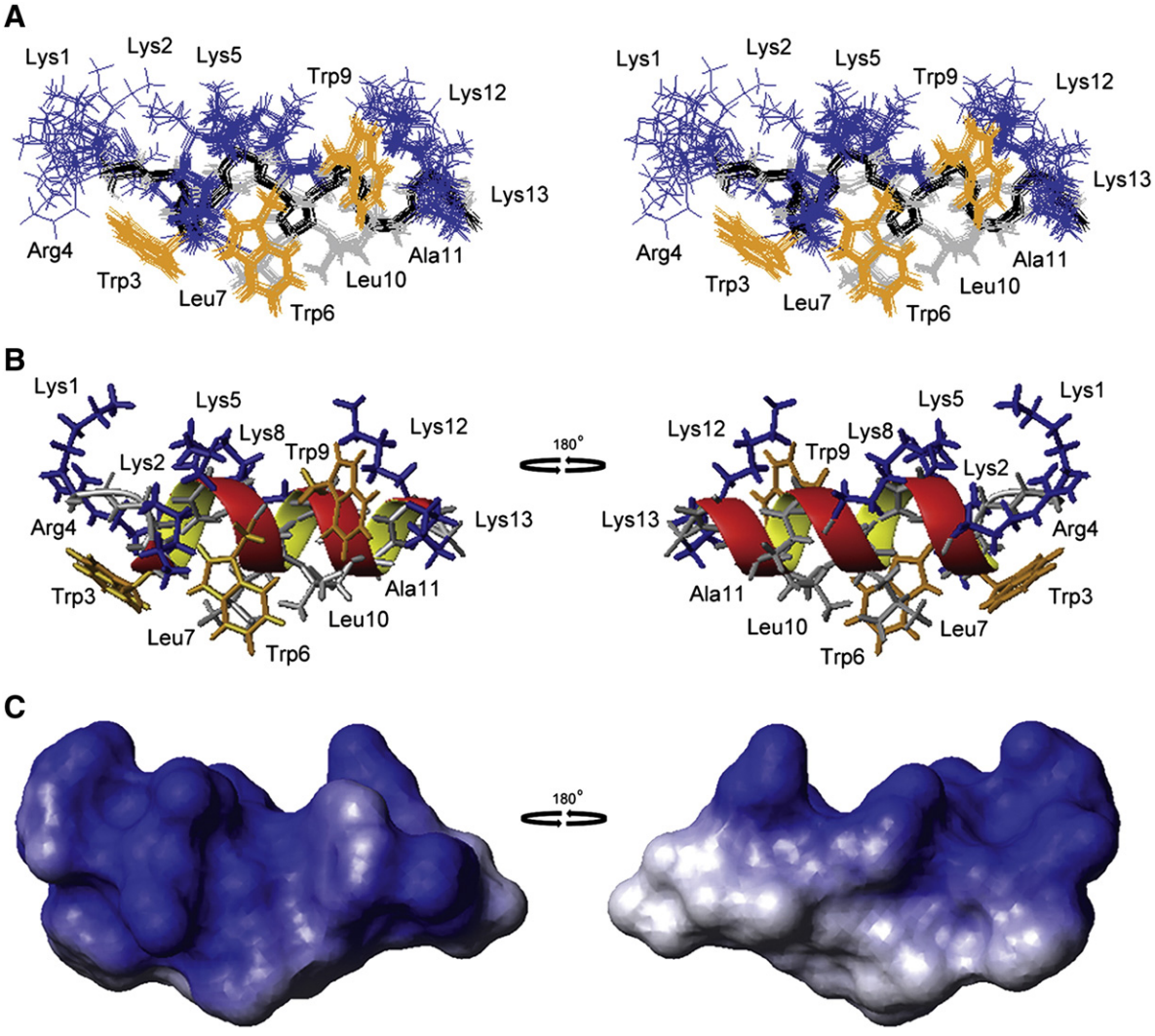

Fig. 1. Calculated structures of PEM-2-W5K/A9W. (A) Stereo-view of 20 lowest energy structures calculated for PEM-2-W5K/A9W. (B) Final refined average structure for PEM-2-W5K/A9W. Positive charged residues are labeled in blue, tryptophan residues are labeled in brown, and hydrophobic residues are labeled in gray. (C) Electrostatic surface plot of PEM-2-W5K/A9W. Positive charge is colored in blue and neutral charge is colored in white.

Table 1
Summary of structural constrains and structure statistics.

NOE restraints	385
Intraresidues (|i–j| = 0)	216
Sequential (|i–j| = 1)	97
Medium range (2≦|i–j|≦4)	72
Energy statistics (kcal/mol)	
Overall	83.84 ± 3.31
Bonds	5.03 ± 0.38
Angles	32.89 ± 1.12
Improper	5.27 ± 0.36
VDW	21.65 ± 5.02
NOE	19.01 ± 1.94
RMSD for geometrical analysis	
Interatomic distances (Å)	0.0042 ± 0.000141
Interatomic angles (degree)	0.643 ± 0.008485
Impropers (degree)	0.465 ± 0.001414
Structural statistics (20 structures)	
NOE violations, number >0.2 (Å)	0
Atomic RMSD for peptide	
All heavy atoms	1.32 ± 0.1
Backbone	0.26 ± 0.37
Ramachandran statistics	
Most favored region (%)	91.4
Additionally allowed (%)	8.6
Generously allowed (%)	0
Disallowed (%)	0

3.2. Orientation in DPC via PRE studies

The orientation of PEM-2 and PEM-2-W5K/A9W in d_{38}-DPC micelles studied by PRE experiments is shown in Fig. 2A. Peak amplitude changes of the NH/Hα cross peaks of the TOCSY spectra of PEM-2 and PEM-2-W5K/A9W in the presence and absence of Gd(DTPA-BMA) and 16-doxylstearic acid are shown in Fig. 2B and C. In general, the remaining cross peak amplitudes of PEM-2 in the presence of Gd(DTPA-BMA) are less than those of PEM-2-W5K/A9W. The remaining cross peak amplitudes of PEM-2 in the presence of 16-doxylstearic acid are larger than those of PEM-2-W5K/A9W. These results indicate that PEM-2 is located at the micelles and water interface, whereas PEM-2-W5K/A9W is inserted deeper into the hydrophobic core of the micelles than PEM-2 is inserted. Based on the PRE studies, the position of each Hα proton and hence the orientation angles of PEM-2 and PEM-2-W5K/A9W can be found to be located within a certain range of degrees onto the surface of d_{38}-DPC-micelles using the program MOLMOL (Fig. 2A).

3.3. Immersion depth in DPC via NOE constraints

Although the orientations of PEM-2 and PEM-2-W5K/A9W on DPC micelles can be determined to a certain degree of accuracy via PRE studies, the immersion depths are needed to be further constrained. Previously, a solution NMR method was developed to determine the orientation of the transmembrane helical peptide TM7 and the antimicrobial peptide CM15 by fitting of the PRE results to the micelle center position [15,23]. Other approach was to measure intermolecular transfer NOE signals between the fatty acyl chain of LPC and the micelle-bound peptide [24]. For PEM-2, intermolecular NOEs were found between the aromatic protons of Trp3, Trp6, and the fatty acyl chain protons of DPC (Fig. 3A). Trp3 and Trp6 are located on the hydrophobic face of PEM-2, whereas Trp5 is located on the hydrophilic face. No intermolecular NOE was detected between Trp5 and the fatty acyl chain protons of DPC. Thus, Trp5 was placed at least 5 Å away from the first CH_2 group of DPC using the program MOLMOL. For Trp6, no NOE was detected between the Hε1 proton of the aromatic ring and the fatty acyl chain protons of DPC. For PEM-2-W5K/A9W, intermolecular NOEs were found between the fatty acyl chain protons of DPC and the aromatic protons of Trp3 (except Hε1), Trp6, and some of the aromatic protons of Trp9 (Hε3, Hξ3, and Hη2) (Fig. 3B). The aromatic protons of Trp3, Trp6, and Trp9 with NOEs were then placed within 5 Å from the CH_2 protons of DPC using the program MOLMOL. By using these NOE restraints and the peak amplitude changes from the PRE experiments, the immersion depths and orientation angles of PEM-2 and PEM-2-W5K/A9W can be determined. Cross-peaks found between the fatty acyl chain protons of DPC micelles (1.325 ppm) and the aromatic protons of tryptophans of PEM-2 and PEM-2-W5K/A9W were listed in Fig. 3C. In addition to the NOEs between the aromatic protons of tryptophans and the acyl chain protons of DPC, we have also observed peaks between water molecules and the NH protons of Lys1, Lys2, and Hε1 proton of Trp5 of PEM-2, and the NH protons of Lys1, Lys2, and Lys5 of PEM-2-W5K/A9W on the hydrophilic face (data not shown). These peaks may arise probably due to chemical exchange between these labile protons and water.

3.4. Confirmation of orientation and immersion depth via saturation transfer difference (STD) NMR studies

STD NMR has been used for a variety of systems including whole viruses, intact cells, micelles, and membrane proteins [25–27]. In here, the intermolecular NOEs between PEM-2, PEM-2-W5K/A9W, and DPC micelles were further confirmed by saturation transfer difference NMR studies. Based on differences between two-dimensional STD TOCSY spectra (on resonance and off resonance), the signals arising from the fatty acyl chain protons of DPC micelles to the aromatic protons of tryptophans of PEM-2 (Fig. 4A) and PEM-2-W5K/A9W (Fig. 4B) were identified. For PEM-2, cross peaks were found for Hδ1, Hε3, Hξ2, Hξ3, Hη2 and aromatic protons of Trp3, Hξ3, Hη2 and aromatic protons of Trp5, and Hδ1, Hε3, Hξ2, Hξ3, Hη2 and aromatic protons of Trp6. For PEM-2-W5K/A9W, cross peaks were found for Hδ1, Hε3, Hξ2, Hξ3, Hη2 and aromatic protons of Trp3, Trp6, and Trp9. No cross peak was found for Hε1 of the tryptophans of PEM-2 and PEM-2-W5K/A9W due to the labile character of these protons under D_2O experimental conditions. The immersion depth and orientation of PEM-2 and PEM-2-W5K/A9W can be determined by combining the results of PRE, NOE, and STD NMR studies using the program MOLMOL (Fig. 5). In Fig. 5, peptides are drawn as ball-and-stick models. Aromatic protons of tryptophans with both NOE and STD cross peaks are represented with red atoms. Aromatic protons of tryptophans with only STD cross peaks are represented with cyan atoms. The results from STD studies matched well with the PRE and intermolecular NOE results.

3.5. Hydrophobic surface areas under DPC micelles

In addition to the immersion depth of PEM-2 and PEM-2-W5K/A9W, we have calculated the hydrophobic surface area buried under DPC micelles for PEM-2 and PEM-2-W5K/A9W using the software PyMol. The results indicate that the hydrophobic surface area for PEM-2 buried under DPC micelles is 584.093 $Å^2$, whereas the hydrophobic surface area for PEM-2-W5K/A9W buried under DPC micelles is 847.654 $Å^2$. The difference of the hydrophobic surface area buried under DPC micelles between PEM-2 and PEM-2-W5K/A9W is 263.561 $Å^2$. However, the surface area of Ala is 69.707 $Å^2$, and the surface area of Trp is 166.116 $Å^2$. The difference of the surface area between Ala and Trp is 96.409 $Å^2$. Thus, the increase of the hydrophobic surface area buried under DPC micelles cannot be attributed only to the replacement of Ala9 with Trp9 in PEM-2-W5K/A9W. It seems that the replacement of Ala9 with Trp9 causes an overall effect on the hydrophobic interactions between the peptide and the acyl chains of DPC micelles and hence makes the peptide buried deeply into the micelles.

3.6. Antimicrobial activities under high salt conditions

PEM-2 and P-113 were used for comparison to demonstrate the efficacy of PEM-2-W5K/A9W against various bacterial and fungal strains under high salt conditions. The MIC values of PEM-2-W5K/A9W were

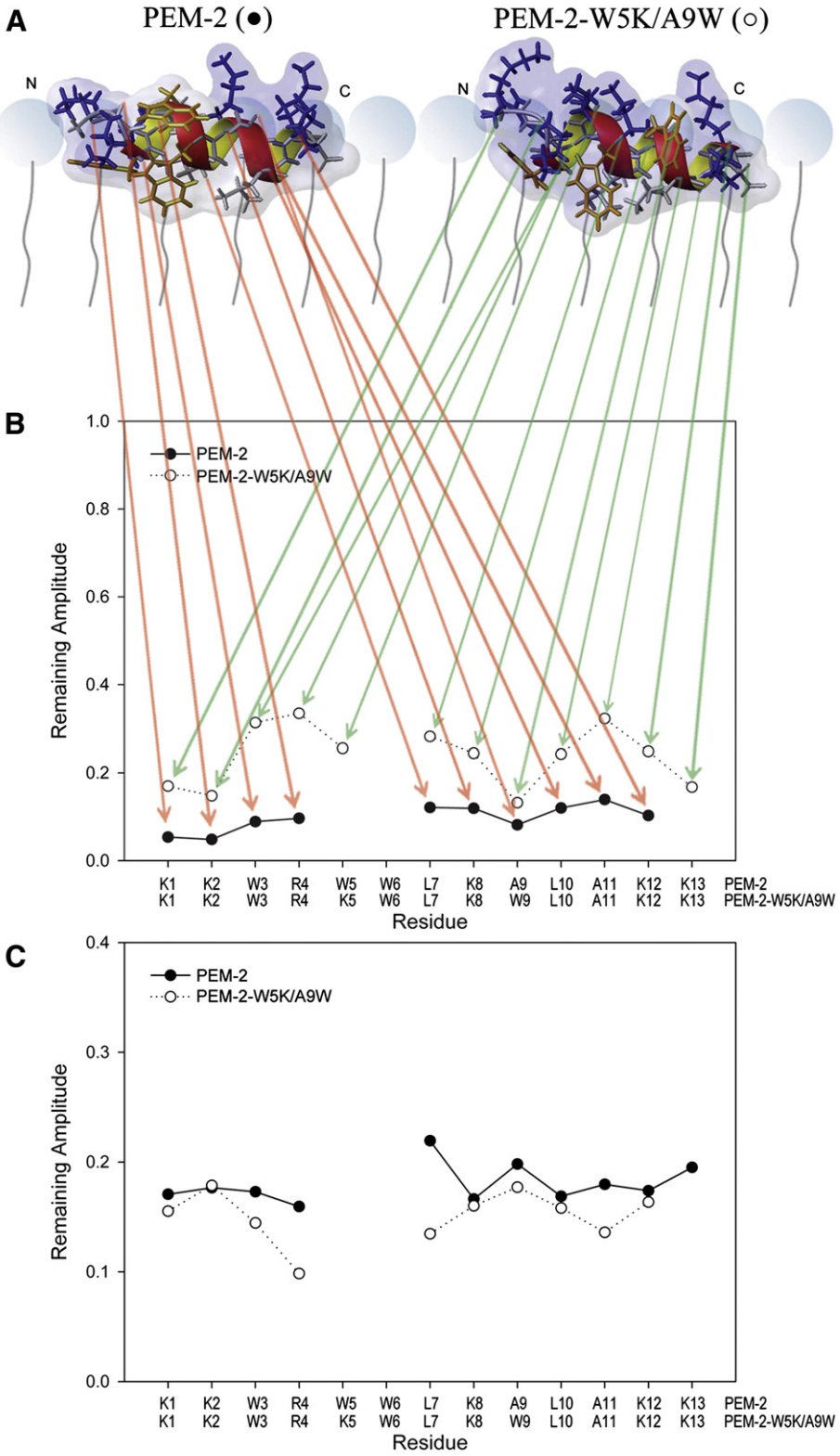

Fig. 2. (A) Immersion depths and orientations of PEM-2 and PEM-2-W5K/A9W buried under DPC micelles. (B) Remaining amplitudes of the NH/Hα cross-peaks in the TOCSY spectra of PEM-2(●) and PEM-2-W5K/A9W (○) in 120 mM d_{38}-DPC and 2 mM Gd(DTPA-BMA). (C) Remaining amplitudes of the NH/Hα cross-peaks in the TOCSY spectra of PEM-2(●) and PEM-2-W5K/A9W (○) in 120 mM d_{38}-DPC and 2 mM 16-doxyl-stearic acid. Missing data points are due to overlapped cross-peaks in the TOCSY spectra.

found to be more potent than PEM-2 and P-113 (Figs. 6 and 7) with only a slightly increase of hemolysis of human red blood cells. Several studies reported that the efficacy of P-113 is greatly reduced in the presence of high salt concentrations [28,29]. As can be found from Fig. 6, PEM-2-W5K/A9W, PEM-2, and P-113 all demonstrate activities against various bacteria strains in the LYM broth media. However, the activity of P-113 and PEM-2 was reduced by the addition of 50 mM NaCl or 0.5 mM $MgCl_2$ into the LYM medium and was further diminished by the addition of 200 mM NaCl or 1.5 mM $MgCl_2$. On the other hand, the MIC values of PEM-2-W5K/A9W were found to be more potent than PEM-

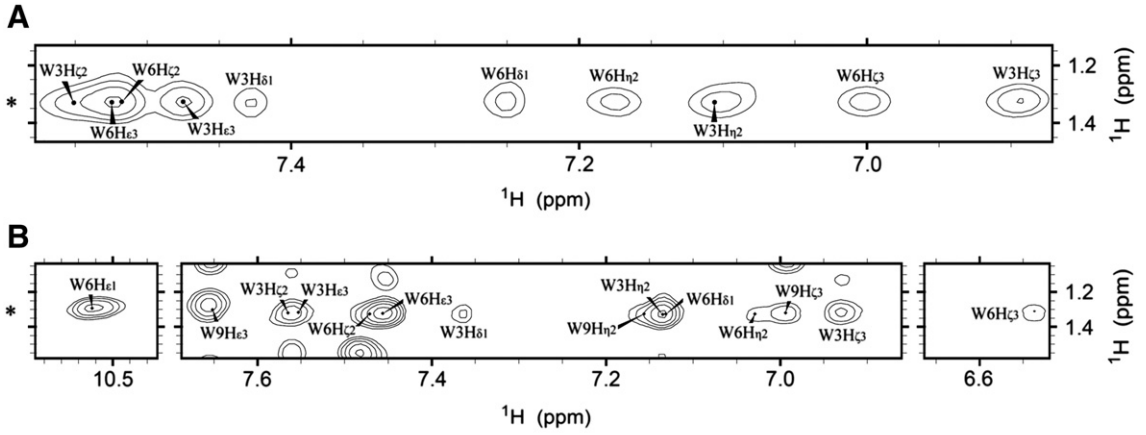

C

Cross-peaks found between the fatty acyl chain protons of DPC micelles (1.325 ppm) and the aromatic protons of tryptophans.

PEM-2	$H_{\delta1}$	$H_{\varepsilon1}$	$H_{\varepsilon3}$	$H_{\zeta2}$	$H_{\zeta3}$	$H_{\eta2}$
Trp-3	V		V	V	V	V
Trp-5						
Trp-6	V		V	V	V	V

PEM-2-W5K/A9W	$H_{\delta1}$	$H_{\varepsilon1}$	$H_{\varepsilon3}$	$H_{\zeta2}$	$H_{\zeta3}$	$H_{\eta2}$
Trp-3	V		V	V	V	V
Trp-6	V	V	V	V	V	V
Trp-9			V		V	V

Cross-peak is denoted with a "V".

Fig. 3. Intermolecular NOEs between the fatty acyl chains of DPC micelles which resonated at 1.325 ppm and the aromatic protons of PEM-2 (A) and PEM-2-W5K/A9W (B). Cross-peaks found between the fatty acyl chain protons of DPC micelles (1.325 ppm) and the aromatic protons of tryptophans were listed (C).

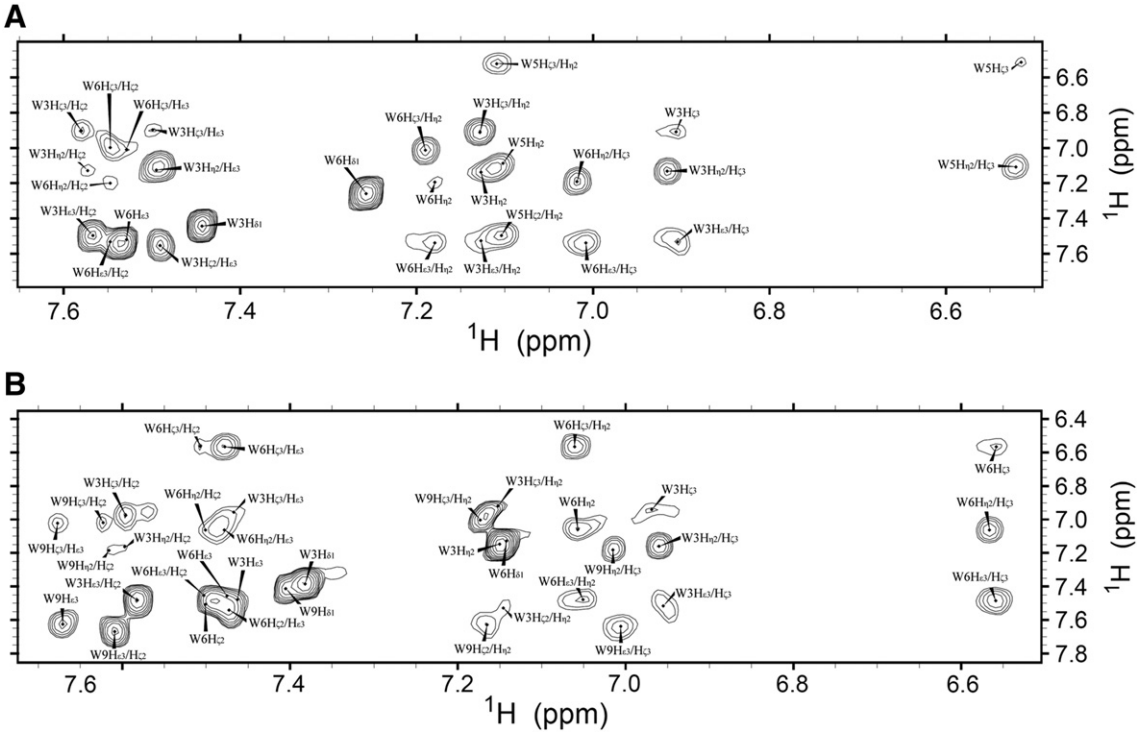

Fig. 4. Saturation transfer difference NMR spectra used to detect cross-peaks between the fatty acyl chains of DPC micelles and the aromatic protons of PEM-2 (A) and PEM-2-W5K/A9W (B).

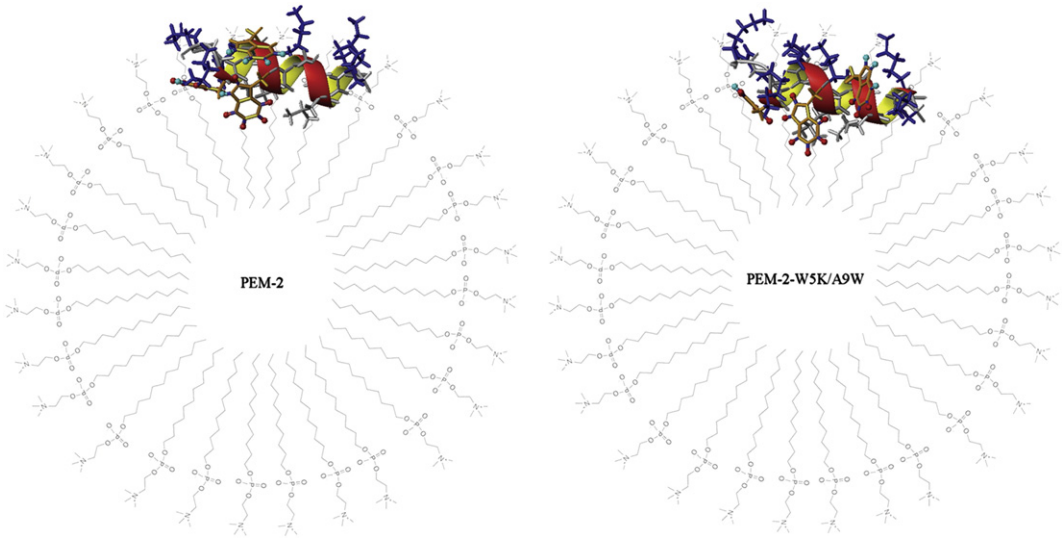

Fig. 5. Immersion depths and orientations of PEM-2 and PEM-2-W5K/A9W buried under DPC micelles based on the PRE, NOE, and STD studies. The hydrophobic surface area for PEM-2 buried under DPC micelles is 584.093 Å^2, whereas the hydrophobic surface area for PEM-2-W5K/A9W buried under DPC micelles is 847.654 Å^2. Peptides are drawn as ball-and-stick models. Aromatic protons of tryptophans with both NOE and STD cross peaks are represented with red atoms. Aromatic protons of tryptophans with only STD cross peaks are represented with cyan atoms.

2 and P-113 in both Mueller–Hinton broth and modified LYM broth media (Fig. 6). PEM-2-W5K/A9W still retained its antibacterial activities with 300 mM NaCl or 2.5 mM $MgCl_2$ added.

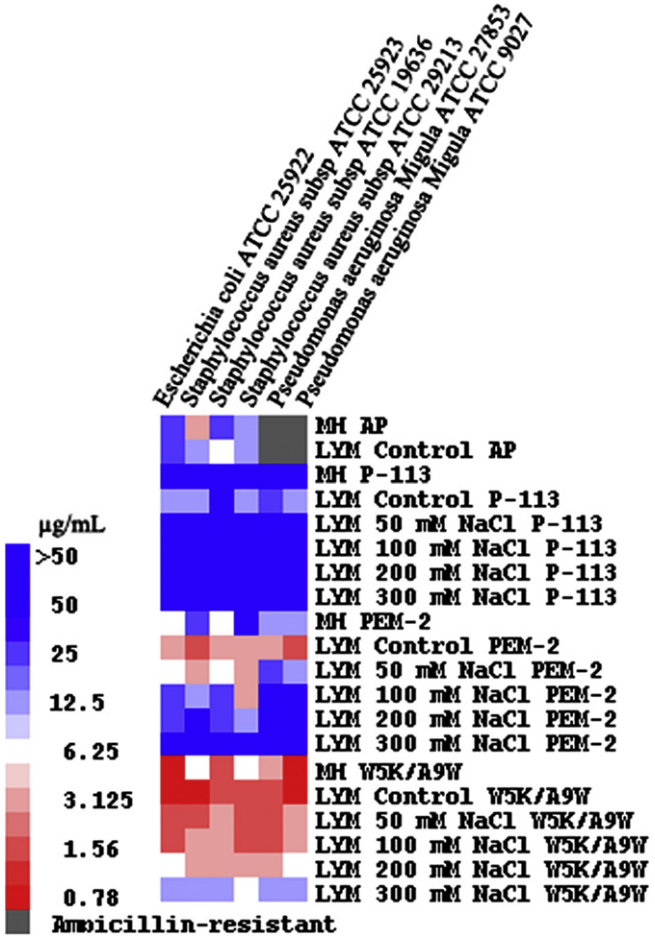

Fig. 6. MIC (anti-bacteria) values displayed on a color scale for Ampicillin (AP), P-113, PEM-2 and PEM-2-W5K/A9W under different concentrations of NaCl.

The anti-Candida activities of fluconazole, P-113, PEM-2, and PEM-2-W5K/A9W were determined in LYM culture media under different salt conditions. There were six resistant strains with high fluconazole MICs (≥32 μg/ml). As expected, P-113, PEM-2, and PEM-2-W5K/A9W all had similar MICs in the LYM medium, ranging from 1.56 to 6.25 μg/ml against yeast pathogens (or Candida species) (Fig. 7). The activity of P-113 was inhibited by the addition of 100 mM NaCl in the LYM medium and that was strongly blocked by the addition of 150 mM NaCl. Similarly, the activity of PEM-2 was reduced with the concentration of NaCl greater than 100 mM. Again, PEM-2-W5K/A9W retained highly active antifungal activities in the media containing 150 mM NaCl (Fig. 7).

4. Discussion

Hydrophobicity has been known as a key factor in the design and development of effective antimicrobial peptides. For example, the number and location of hydrophobic residues, as well as their hydrophobicity and type of hydrophobe are important factors that can affect the antimicrobial activities of amphipathic α-helical peptides [30,31]. In addition, a balance of the hydrophobicity and charge distribution of antimicrobial peptides can generate effective antibacterial activities without cytotoxicity to mammalian cells [32]. However, less has been addressed in the involvement of hydrophobicity in the development of salt-resistant antimicrobial peptides.

Recently we have developed an easy strategy to increase salt resistance of antimicrobial peptides by replacing tryptophan or histidine residues with the bulky amino acid β-naphthylalanine [6]. The β-naphthylalanine replacements may help these peptides to penetrate deeper into the bacterial and fungal cell membranes, hence making these peptides more efficient in disrupting the membranes. However, relationships between the increased hydrophobic surface areas of the non-natural amino acids, membrane immersion depth, orientation, and salt-resistance of these peptides are still unknown. In this study, we have determined the solution structure of the Trp-rich antimicrobial peptide PEM-2-W5K/A9W, and studied its paramagnetic relaxation enhancement in DPC micelles. The solution structure of PEM-2-W5K/A9W is very similar to the structure of PEM-2. Thus, the replacements of the amino acids did not change the peptide backbone structure. PRE and NOE studies indicate that PEM-2-W5K/A9W can insert more deeply into the DPC micelles

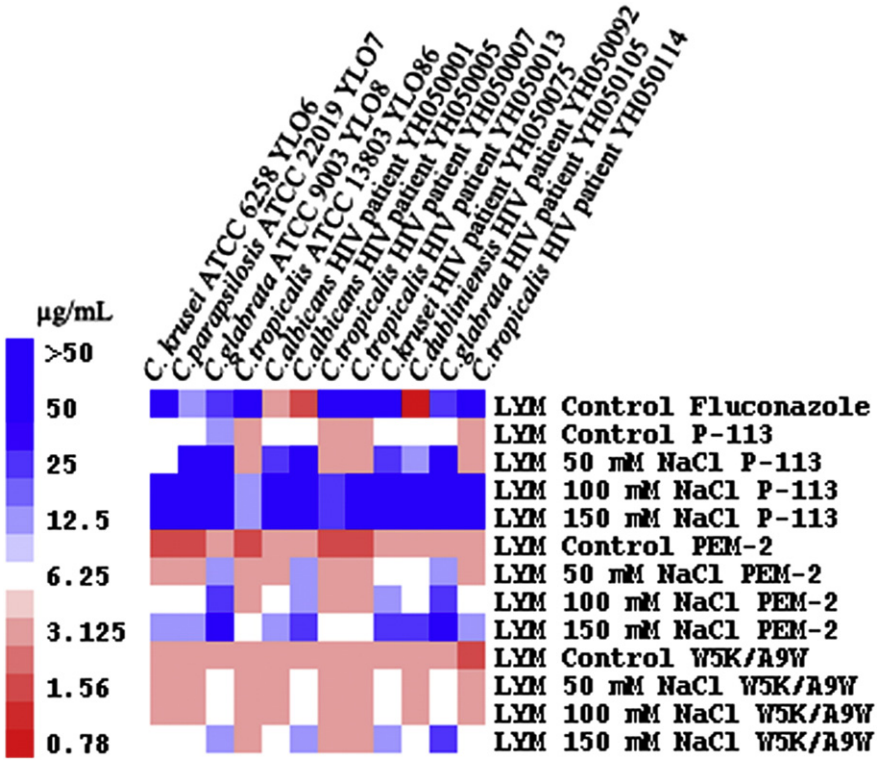

Fig. 7. MIC (anti-Candida) values displayed on a color scale for fluconazole, P-113, PEM-2 and PEM-2-W5K/A9W under different concentrations of NaCl.

and possess a larger buried hydrophobic surface than its parent peptide PEM-2. Similar to the β-naphthylalanine substitutions [6], the replacement of Trp5 and Ala9 by Lys and Trp of PEM-2 makes PEM-2-W5K/A9W to have a larger hydrophobic surface buried under DPC micelles. These results showed a direct relationship between membrane-bound surface area and salt-resistance of antimicrobial peptides. This correlation may be useful to design salt-resistant antimicrobial peptides. For example, membrane-bound surface area can be increased by replacing tryptophan or histidine residues with non-natural bulky amino acids [33,34], by adding hydrophobic oligopeptide end tags [35–37], or by adding fatty acid, vitamin E, or cholesterol to the termini of antimicrobial peptides [19,38–41].

Increasing hydrophobicity of antimicrobial peptides also leads to a higher hemolytic activity. This has been observed in the β-naphthylalanine substituted Trp-rich antimicrobial peptides [33,34] and other studies [31]. This problem may be compensated by increasing the positive charge residues on the hydrophilic face of the antimicrobial peptides [31]. To test this idea, we have studied PEM-2-W5A/A9W, with only Trp5 and Ala9 swapping positions. PEM-2-W5A/A9W demonstrates similar salt-resistance in comparison with PEM-2-W5K/A9W (data not shown). This may be due to the fact that Ala9 in the hydrophobic face was replaced by a larger Trp residue in both peptides. However, PEM-2-W5A/A9W has a higher hemolytic activity than PEM-2-W5K/A9W has. The only difference is there is a Lys instead of an Ala residue on the hydrophilic face of PEM-2-W5K/A9W. Similar result has been observed where the number and location of positively charged residues on the hydrophilic face can have a large effect on hemolytic and antimicrobial activities [31].

With the emergence of antibiotic resistant microbes, the need for the development of novel therapeutics has become an increasingly important issue. Certain antimicrobial peptides containing potent and broad-spectrum activities against various microbial pathogens are already in clinical trials [1]. However, the antimicrobial activities of some agents were found to diminish under physiological and high salt conditions [11,42,43]. In this study, the Trp-rich peptide, PEM-2-W5K/A9W, has potent activity against microbial pathogens, including methicillin, ampicillin, and fluconazole resistant strains. Moreover, the antimicrobial activity is no longer hindered by high salt concentrations.

Acknowledgement

We thank Dr. Hsiu-Jung Lo of National Health Research Institute for her help in the anti-Candida experiments. This work is supported by grants from National Science Council, Taiwan. Bak-Sau Yip was supported by a research grant from the National Taiwan University Hospital Hsinchu Branch.

Appendix A. Supplementary data

Supplementary data to this article can be found online at http://dx.doi.org/10.1016/j.bbamem.2013.07.020.

References

[1] R.E.W. Hancock, H.G. Sahl, Antimicrobial and host-defense peptides as new anti-infective therapeutic strategies, Nat. Biotechnol. 24 (2006) 1551–1557.
[2] I.Y. Park, J.H. Cho, K.S. Kim, Y.B. Kim, M.S. Kim, S.C. Kim, Helix stability confers salt resistance upon helical antimicrobial peptides, J. Biol. Chem. 279 (2004) 13896–13901.
[3] M.J. Goldman, G.M. Anderson, E.D. Stolzenberg, U.P. Kari, M. Zasloff, J.M. Wilson, Human b-defensin-1 is a salt-sensitive antibiotic in lung that is inactivated in cystic fibrosis, Cell 88 (1997) 553–560.
[4] I.H. Lee, Y. Cho, R.I. Lehrer, Effects of pH and salinity on the antimicrobial properties of clavanins, Infect. Immun. 65 (1997) 2898–2903.
[5] D.M. Rothstein, P. Spacciapoli, L.T. Tran, T. Xu, F.D. Roberts, M. Dalla Serra, D.K. Buxton, F.G. Oppenheim, P. Friden, Anticandida activity is retained in P-113, a 12-amino-acid fragment of histatin 5, Antimicrob. Agents Chemother. 45 (2001) 1367–1373.
[6] C.W. Wang, B.S. Yip, H.T. Cheng, A.H. Wang, H.L. Chen, J.W. Cheng, H.J. Lo, Increased potency of a novel D-b-naphthylalanine-substituted antimicrobial peptide against fluconazole-resistant fungal pathogens, FEMS Yeast Res. 9 (2009) 967–970.
[7] M. Wu, E. Maier, R. Benz, R.E.W. Hancock, Mechanism of interaction of different classes of cationic antimicrobial peptides with planar bilayers and with the cytoplasmic membrane of *Escherichia coli*, Biochemistry 38 (1999) 7235–7242.
[8] B. Deslousches, S.M. Phadke, V. Lazarevic, M. Cascio, K. Islam, R.C. Montelaro, T.A. Mietzner, De novo generation of cationic antimicrobial peptides: influence of length and tryptophan substitution on antimicrobial activity, Antimicrob. Agents Chemother. 49 (2005) 316–322.

[9] C. Friedrich, M.G. Scott, N. Karunaratne, H. Yan, R.E.W. Hancock, Salt-resistant alpha-helical cationic antimicrobial peptides, Antimicrob. Agents Chemother. 43 (1999) 1542–1548.
[10] S.S.L. Harwig, A. Waring, H.J. Yang, Y. Cho, L. Tan, R.I. Lehrer, Intramolecular disulfide bonds enhance the antimicrobial and lytic activities of protegrins at physiological sodium chloride concentrations, Eur. J. Biochem. 240 (1996) 352–357.
[11] T. Rydlo, S. Rotem, A. Mor, Antibacterial properties of Dermaseptin S4 derivatives under extreme incubation conditoins, Antimicrob. Agents Chemother. 50 (2006) 490–497.
[12] J.P. Tam, Y.A. Lu, J.L. Yang, Design of salt-insensitive glycine-rich antimicrobial peptides with cyclic tricystine structures, Biochemistry 39 (2000) 7159–7169.
[13] C. Santamaria, S. Larios, Y. Angulo, J. Pizarro-Cerda, J.P. Gorvel, E. Moreno, B. Lomonte, Antimicrobial activity of myotoxic phospholipases A_2 from crotalid snake venoms and synthetic peptide variants derived from their C-terminal region, Toxicon 45 (2005) 807–815.
[14] H.Y. Yu, K.C. Huang, B.S. Yip, C.H. Tu, H.L. Chen, H.T. Cheng, J.W. Cheng, Rational design of tryptophan-rich antimicrobial peptides with enhanced antimicrobial activities and specificities, ChemBioChem 11 (2010) 2273–2282.
[15] M. Respondek, T. Madl, C. Gobl, R. Golser, K. Zangger, Mapping the orientation of helices in micelle-bound peptides by paramagnetic relaxation waves, J. Am. Chem. Soc. 129 (2007) 5228–5234.
[16] F. Abbassi, O. Lequin, C. Piesse, N. Goasdoue, T. Foulon, P. Nicolas, A. Ladram, Temporin-SHf, a new type of Phe-rich and hydrophobic ultrashort antimicrobial peptide, J. Biol. Chem. 285 (2010) 16880–16892.
[17] A. Carotenuto, S. Malfi, M.R. Saviello, P. Campiglia, I. Gomez-Monterrey, M.L. Mangoni, L.M.H. Gaddi, E. Novellino, P. Grieco, A different molecular mechanism underlying antimicrobial and hemolytic actions of temporins A and L, J. Med. Chem. 51 (2008) 2354–2362.
[18] R.A. Laskowski, J.A. Rullmannn, M.W. MacArthur, R. Kaptein, J.M. Thornton, AQUA and PROCHECK-NMR: programs for checking the quality of protein structures solved by NMR, J. Biomol. NMR 8 (1996) 477–486.
[19] C.J. Arnusch, H. Ulm, M. Josten, Y. Shadkchan, N. Osherov, H.G. Sahl, Y. Shai, Ultrashort peptide bioconjugates are exclusively antifungal agents and synergize with cyclodextrin and amphotericin B, Antimicrob. Agents Chemother. 56 (2012) 1–9.
[20] M.B. Eisen, P.T. Spellman, P.O. Brown, D. Botstein, Cluster analysis and display of genome-wide expression patterns, Proc. Natl. Acad. Sci. 95 (1998) 14863–14868.
[21] S.Y. Wei, J.M. Wu, Y.Y. Kuo, H.L. Chen, B.S. Yip, S.R. Tzeng, J.W. Cheng, Solution structure of a novel tryptophan-rich peptide with bidirectional antimicrobial activity, J. Bacteriol. 188 (2006) 328–334.
[22] K. Wuthrich, NMR of Proteins and Nucleic Acids, John Wiley & Sons, New York, USA, 1986.
[23] K. Zangger, M. Respondek, C. Gobl, W. Hohlweg, K. Rasmussen, G. Grampp, T. Madl, Positioning of micelle-bound peptides by paramagnetic relaxation enhancements, J. Phys. Chem. B 113 (2009) 4400–4406.
[24] W.N. Huang, S.C. Sue, D.S. Wang, P.L. Wu, W.G. Wu, Peripheral binding mode and penetration depth of cobra cardiotoxin on phospholipid membranes as studied by a combined FTIR and computer simulation approach, Biochemistry 42 (2003) 7457–7466.
[25] A. Bhunia, S. Bhattacharjya, S. Chatterjee, Applications of saturation transfer difference NMR in biological systems, Drug Discov. Today (Dec. 2011) 1–9.
[26] A. Bhunia, P.N. Domadia, J. Torres, K.J. Hallock, A. Ramamoorthy, S. Bhattacharjya, NMR structure of pardaxin, a pore-forming antimicrobial peptide, in lipopolysaccharide micelles, J. Biol. Chem. 285 (2010) 3883–3895.
[27] A. Bhunia, R. Saravanan, H. Mohanram, M.L. Mangoni, S. Bhattacharjya, NMR structures and interactions of temporin-1TI and temporin-1Tb with lipopolysaccharide micelles, J. Biol. Chem. 286 (2011) 24394–24406.
[28] E.J. Helmerhorst, W. Van T Hof, E.C.I. Veerman, I. Simmons-Smit, A.V. Nieuw Amerongen, Synthetic histatin analogues with broad-spectrum antimicrobial activity, Biochem. J. 326 (1997) 39–45.
[29] W.S. Jang, X.S. Li, J.N. Sun, M. Edgerton, The P-113 fragment of histatin 5 requires a specific peptide sequence for intracellular translocation in *Candida albicans*, which is independent of cell wall binding, Antimicrob. Agents Chemother. 52 (2008) 497–504.
[30] Y. Chen, M.T. Guarnieri, A.I. Vasil, M.L. Vasil, C.T. Mant, R.S. Hodges, Role of peptide hydrophobicity in the mechanism of action of a-helical antimicrobial peptides, Antimicrob. Agents Chemother. 51 (2007) 1398–1406.
[31] Z. Jiang, A.I. Vasil, L. Gera, M.L. Vasil, R.S. Hodges, Rational design of a-helical antimicrobial peptides to target gram-negative pathogens, *Acinetobacter baumannii* and *Pseudomonas aeruginosa*: utilization of charge, 'specificity determinants', total hydrophobicity, hydrophobe type and location as design parameters to improve the therapeutic ratio, Chem. Biol. Drug Des. 77 (2011) 225–240.
[32] L.M. Yin, M.A. Edwards, J. Li, C.M. Yip, C.M. Deber, Roles of hydrophobicity and charge distribution of cationic antimicrobial peptides in peptide–membrane interactions, J. Biol. Chem. 287 (2012) 7738–7745.
[33] J.M. Wu, S.Y. Wei, H.L. Chen, K.Y. Weng, H.T. Cheng, J.W. Cheng, Solution structure of a novel D-naphthylalanine substituted peptide with potential antibacterial and antifungal activities, Biopolymers 88 (2007) 738–745.
[34] H.Y. Yu, C.H. Tu, B.S. Yip, H.L. Chen, H.T. Cheng, K.C. Huang, H.J. Lo, J.W. Cheng, Easy strategy to increase salt resistance of antimicrobial peptides, Antimicrob. Agents Chemother. 55 (2011) 4918–4921.
[35] M. Pasupuleti, A. Chalupka, M. Morgelin, A. Schmidtchen, M. Malmsten, Tryptophan end-tagging of antimicrobial peptides for increased potency against *Pseudomonas aeruginosa*, Biochim. Biophys. Acta 1790 (2009) 800–808.
[36] M. Pasupuleti, A. Schmidtchen, A. Chalupka, L. Ringstad, M. Malmsten, End-tagging of ultra-short antimicrobial peptides by W/F stretches to facilitate bacterial killing, PLoS One 4 (2009) e5285.
[37] A. Schmidtchen, M. Pasupuleti, M. Morgelin, M. Davoudi, J. Alenfall, A. Chalupka, M. Malmsten, Boosting antimicrobial peptides by hydrophobic oligopeptide end tags, J. Biol. Chem. 284 (2009) 17584–17594.
[38] D. Avrahami, Y. Shai, Conjugation of a magainin analogue with lipophilic acids controls hydrophobicity, solution assembly, and cell selectivity, Biochemistry 41 (2002) 2254–2263.
[39] A. Makovitzki, D. Avrahami, Y. Shai, Ultrashort antibacterial and antifungal lipopeptides, Proc. Natl. Acad. Sci. 103 (2006) 15997–16002.
[40] Y. Rosenfeld, N. Lev, Y. Shai, Effect of the hydrophobicity to net positive charge ratio on antibacterial and anti-endotoxin activities of structurally similar antimicrobial peptides, Biochemistry 49 (2010) 853–861.
[41] G.N. Serrano, G.G. Zhanel, F. Schweizer, Antibacterial activity of ultrashort cationic Lipo-b-peptides, Antimicrob. Agents Chemother. 53 (2009) 2215–2217.
[42] B. Deslousches, K. Islam, J.K. Craigo, S.M. Paranjape, R.C. Montelaro, T.A. Mietzner, Activity of the de novo engineered antimicrobial peptide WLBU2 against peudomonas aeruginosa in human serum and whole blood: implications for systemic applications, Antimicrob. Agents Chemother. 49 (2005) 3208–3216.
[43] L. Zhang, J. Parente, S.M. Harris, D.E. Woods, R.E.W. Hancock, T.J. Falla, Antimicrobial peptide therapeutics for cystic fibrosis, Antimicrob. Agents Chemother. 49 (2005) 2921–2927.